Engineering and Applied Science Research 2024;51(6):800-809 Research Article

EASR

Engineering and Applied Science Research

https://www.tci-thaijo.org/index.php/easr/index

Published by the Faculty of Engineering, Khon Kaen University, Thailand

Mineralogical-based rock abrasivity assessment of siliciclastic and carbonate rocks observed in Mae Moh District, northern Thailand

Nat Setteetorn and Tadsuda Taksavasu*

Department of Mining and Petroleum Engineering, Faculty of Engineering, Chiang Mai University, Chiang Mai 50200, Thailand

Received 24 July 2024
Revised 26 November 2024
Accepted 28 November 2024

Abstract

Understanding a target rock's characteristics and tool wear behaviors after cutting that rock significantly leads to appropriate tool selections and reliable tool lifetime prediction for ground excavation or drilling activities in mining and construction industries. Rock abrasivity is defined as the ability of rocks to cause damage to cutting tools. There are several methods for investigating the abrasivity of rocks ranging from micro-scale geotechnical approaches to real-scale in-situ tests. Applying mineralogical analysis to the rock abrasivity assessment methods for the tool wear prediction is lacking in detail, despite its simplicity, effectiveness, and affordability. This study preliminarily tests the abrasivity of four stratigraphic sedimentary units hosted in the Mae Moh Basin, northern Thailand, by investigating a rock abrasivity index (RAI). The method involves microscopic petrographic analysis, equivalent quartz content (EQC) determination, and the uniaxial compressive strength (UCS) tests. The RAI of each representative rock unit is a product of its EQC and UCS. The petrographic results reveal that the rock samples are sandstones and limestones. The sandstones can be divided into two subtypes including sublithic and lithic arenites with the EQC of 90.3% and 43.3%, respectively. The limestones, on the other hand, show the opposite values of below 3%. The UCS results suggest that the strengths of sandstones are higher than limestones. Additionally, the lithic-rich sandstone shows the highest UCS value (92.2 MPa). The calculated RAI of sandstones ranges from 39.9 to 72.5, indicating medium-to-very abrasive materials, whereas the limestones show RAI values of less than 2, indicating non-abrasive rocks. Determination of rock abrasivity using its mechanical and mineralogical properties appears to be a practical method for drilling or excavation strategies.

Keywords: Equivalent quartz content, Petrography, Rock abrasivity index, Rosiwal hardness, Tool wear prediction

1. Introduction

The potential of rocks or rock mass to wear or erode metal surfaces of excavation or drilling tools has been referred to as rock abrasivity. It is one of the key parameters for mining and underground construction applications, to determine the tool performance, such as speed and lifetime, and to estimate the operating costs [1-4]. Rock abrasivity can be investigated on various scales, from microscopic analytical techniques to real-scale field site testing procedures [e.g. 5-13]. Focusing on micro-scale geotechnical approaches, a rock abrasivity index (RAI) has been proposed by Plinninger since 2002 [5, 6]. It is obtained from a combination of mineralogical and mechanical input parameters of a rock that involves its equivalent quartz content (EQC) and uniaxial compressive strength (UCS) [5, 12]. This method has been considered an affordable and fast way of determining rock abrasivity as it involves parameters, which are common and reliable worldwide [5, 6, 10].

One of the major causes of tool wear has been proposed as mineral or rock hardness [14-16]. The EQC stands for the entire mineral content referring to the hardness of quartz based on the Rosiwal grinding hardness [5, 17-20]. The mineralogical content of rocks can be investigated by a thin-section analysis using an optical petrographic microscope. This technique is suitable for hand specimens, rock cuttings, or chippings. The modal rock-forming mineral composition and its textures are observed and interpreted on a microscopic scale. Another alternative technique for mineral and crystal identification has been known as the X-ray powdered diffraction (XRD) method, which appears to be sufficient at some points, especially when the standard petrographic analysis cannot be applicable.

Another crucial parameter influencing tool wear is referred to the strength of the rock, which is commonly indicated by the UCS values. The rock strength is typically controlled by mineral composition, texture, structure, bedding, water content, and state of stress in the rock mass [21]. The UCS can be obtained by various testing standards, whether the International Society for Rock Mechanics (ISRM) or American Standards for Testing and Materials (ASTM) suggested methods [10, 22, 23]. When the standard UCS tests cannot be conducted, another option for determining the rock strength is known as indirect testing methods, including a point load test and a Schmidt hammer test [e.g. 10, 24].

The RAI distinctly varies among geologic formations due to discrete mineral composition, mineral hardness, rock texture, orientation, and/or rock strength. According to previous experiments from Plinninger [5, 10], the RAI of sedimentary rocks generally ranges from 0 to 150. Siliceous sandstones and conglomerates exhibit relatively high RAI compared to limestones and mudstones. Basalts and granites have the RAI range of 15–40 and 10–70, respectively. The RAI of metamorphic rocks, on the other hand, show a

*Corresponding author.
Email address: tadsuda.t@cmu.ac.th
doi: 10.14456/easr.2024.75

wide range of values (<10–360). The highest RAI value reported by the previous works was determined from quartzites [5, 10]. A classification of RAI has also been first introduced in 2002 with five categories, ranging from not abrasive to extremely abrasive. The uses of RAI for estimating the wear of button bits and predicting the drill-bit lifetime have increased in geotechnical engineering contractors [5, 10, 25]. However, there is a lack of research relating to the rock abrasivity assessment using the application of RAI available in Thailand.

This study aims to assess the rock abrasivity of representative sedimentary rocks in the lower formations of the Lampang Group located in northern Thailand, by using the mineralogical-based investigation. The rock units including sandstones and limestones are mineralogically interpreted through a conventional petrographic analysis and mechanically tested for rock strength by a UCS testing method. The study additionally provides the calculated EQC, UCS, and ultimately RAI of each unit. These parameters measured from different rocks are also compared and discussed.

2. Materials and methods

2.1 Rock sampling and description

The rock samples were collected from several locations in the Mae Moh and Mae Tha districts of Lampang province with coordinates as shown in Table 1. The samples exhibit various sedimentary rocks, which come from exposed outcrops and rock floats of the lower four formations of the Lampang Group, including Phra That sandstone (Tr_1), Pha Kan limestone (Tr_2), Hong Hoi sandstone (Tr_3), and Doi Long limestone (Tr_4). Detailed lithologic descriptions of each sample have been provided in the next section.

2.2 Petrographic interpretation

The specimens were individually prepared as a thin section having a dimension of approximately 24×40 mm^2 with a thickness of 0.03 mm. About 8 thin sections were examined under a polarized light using a conventional petrographic microscope. The samples were microscopically observed and described based on their mineralogy and textural characteristics. The modal mineralogical composition of each section was interpreted by a 400-point counting method.

Table 1 Rock sampling locations and rock unit descriptions provided by previous literature [26-28]

Sample ID (Formation Name)	Sampling Location: Northing	Sampling Location: Easting	Rock unit description
Tr_1 (Phra That)	18.3131501	99.6549433	Red beds of conglomerates, sandstones, siltstones, mudstones
Tr_2 (Pha Kan)	18.3133379	99.6559206	Shallow marine limestones
Tr_3 (Hong Hoi)	18.3576250	99.7631751	Fine-grained turbidites; mudstones, sandstones, shale conglomerates, siltstones
Tr_4 (Doi Long)	18.3087283	99.6880833	Shallow marine limestones and dolomitic limestones

2.3 Uniaxial compressive strength test

The rock strength testing method was conducted using a uniaxial compressive strength machine at the Department of Mining and Petroleum Engineering, Chiang Mai University, following the standard testing method of ASTM D 2938-95 [23]. The remaining specimens were prepared as core samples using a core drilling technique. The testing procedure involves (i) placing a core sample into a testing chamber with a vertical axis, and (ii) applying a load at the top area of the core sample with a loading rate of 70–90 kPa per second. The working system was stopped once the core sample broke down as the rock failure occurred. The recent load, in which the failure occurred, was recorded as the maximum load (P). Three core samples from each formation were produced and tested.

2.4 Calculations of the related parameters

Starting with the mineral assemblages and their modal contents, the equivalent quartz content (EQC) of each sample was determined using equation 1 as shown in Table 2. The EQC refers to a sum of multiplied products between a modal percent of each mineral observed in a thin section and its Rosiwal grinding hardness value [6, 10]. This study has distinctly adopted the relationships between the Rosiwal and Mohs scale hardness through equation 2 presented in Table 2 [19]. For instance, quartz has a Mohs scale of 7 that indicates a value of 104.33 for its Rosiwal hardness. On the other hand, the Mohs scale of calcite is 3 suggesting the value of 2.31 for its Rosiwal hardness.

According to the rock strength calculation, the maximum load of each core slab was subdivided by the core internal cross-section area, resulting in the UCS value (equation 3 in Table 2). Each formation provides at least three UCS values. Its UCS average value was used for calculating a rock abrasivity index (RAI) by multiplying with its EQC as presented in equation 4 (Table 2).

Table 2 Equations relating to the rock abrasivity index calculation used in this study

No.	Equations	Parameter definition and unit
(1)	$EQC = \sum_{i=1}^{n} A_i \cdot R_i$	EQC = *Equivalent Quartz Content* (%) A_i = *A mineral content* (%) R_i *or* R = *Rosiwal grinding hardness of a mineral* (%)
(2)	$M = 2.12 + 1.05\, ln(R)$	n = *Total number of minerals in the sample*
(3)	$\sigma_{UCS} = \frac{P}{A}$	M = *Mohs scale of a mineral hardness*
(4)	$RAI = EQC \cdot UCS$	σ_{UCS} *or* UCS = *Uniaxial Compressive Strength* (MPa) P= *Force failure or maximum load applied to the sample* (kN) A = *Initial cross-section area of the core slab* (mm²) RAI = *Rock Abrasivity Index*

Based on previous works, the values of RAI are unitless and have been classified into five classes as shown in Table 3 [8, 10]. Higher RAI values refer to higher abrasive tolerance of the rocks that affect extreme tool wear. The results of these calculations are then interpreted in terms of mineralogical relationships between rock type and rock strength.

Table 3 Rock abrasivity classification based on RAI values [8, 10]

RAI Value	Classification	Tool wear
< 10	Not Abrasive	Low
10 – 30	Slightly Abrasive	
30 – 60	Medium Abrasive	
60 – 120	Very Abrasive	
> 120	Extremely Abrasive	High

3. Results and discussion

3.1 Lithological description

In general, the studied samples exhibit a pair of sedimentary rock features, which comprise clastic sandstones of Tr_1 (Phra That) and Tr_3 (Hong Hoi) and limestones of Tr_2 (Pha Kan) and Tr_4 (Doi Long) as presented in Figure 1. Tr_1 sandstone exhibits white-to-light brown color with coarse-to-medium grain sizes, while Tr_3 sandstone shows greenish grey to grey colors with coarse grain sizes associated with variable volcanic clasts. The Tr_2 limestone exhibits grey to light brown with very fine-grained textures. Tr_4 limestone shows identical color ranges to the Tr_2. Both limestone formations are crosscut by several-stage calcite veins or veinlets.

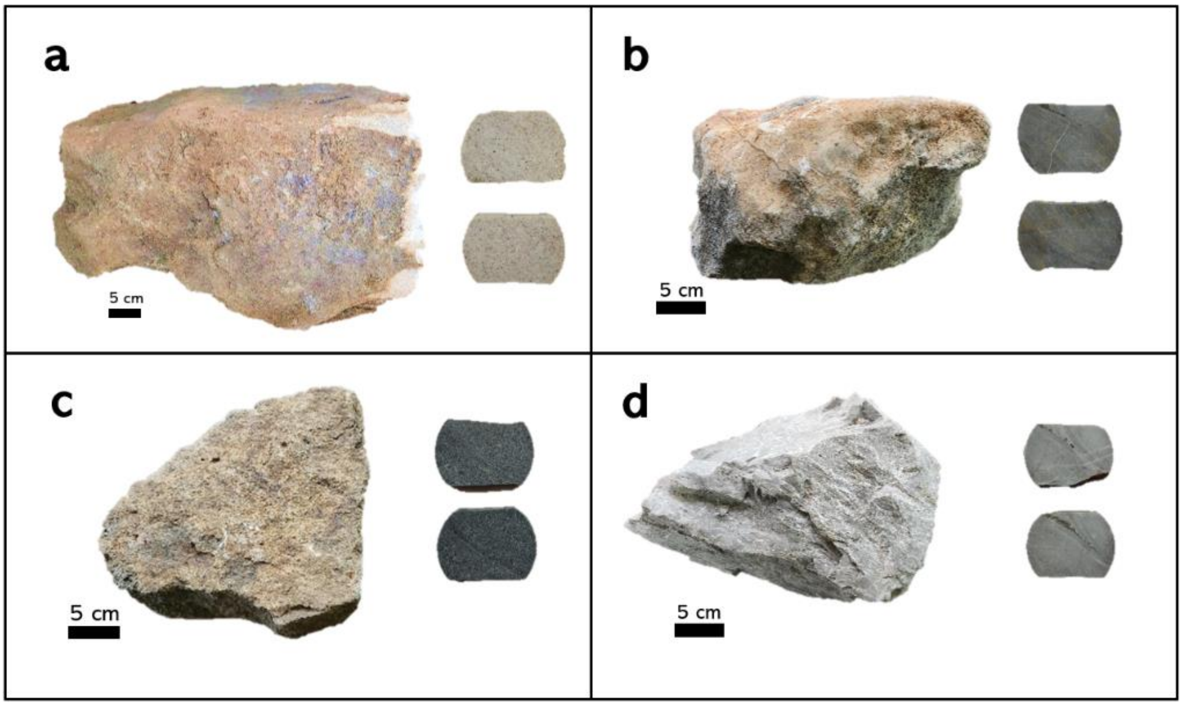

Figure 1 Rock samples representing the formations of Lampang Group occurred in Mae Moh Basin including (a) Tr_1 white sandstone, (b) Tr_2 limestone, (c) Tr_3 green sandstone, and (d) Tr_4 limestone

3.2 Petrographic interpretation

Under microscopic views, the Tr_1 samples exhibit clast-supported fabric textures with moderate sorting. Most grain shapes are angular-to-subround, having high sphericity with an average grain size of 0.1–2 mm (Figure 2). This grain-size range refers to a very coarse-to-fine sand. The rock samples consist of 78–81.25% clasts, 2.5–5.25% matrix, and 5.5–5.75% silica cement associated with 10.5–11.25% secondary phases, such as quartz veins and sericite. More than 60% of the components are undulatory quartz forming as monocrystalline and polycrystalline. Alkali feldspar clasts are observed in approximately 6.625%, whereas lithic (rock) fragments are observed in 8.125%. The lithic fragments comprise clasts of siliceous rocks (3.875%), volcanic-to-pyroclastic rocks (2.375%), and schists/phyllites (1.875%). According to the classifications by Pettijohn [29], the primary mineral component of the samples indicates an arenite group of sandstones. Based on the clast types, it has been classified as a sublitharenite-to-subarkose sandstone.

Tr_2 is mainly composed of 66–78.25% carbonate matrixes (micrites) associated with 0.75–2.75% carbonate cements (sparites) as shown in Figure 3. The carbonate clasts or allochems have not been found as primary components. Around 18.25–27.75% of the whole rock are recrystallized dolomite grains having an average grain size of 0.01–0.03 mm. Secondary carbonate minerals (2.75–3.5%) are also observed to form as veins exhibiting thicknesses of up to 0.4 mm. Reddish-brown iron hydroxide (possibly FeOOH) coating on carbonate grains has locally been observed. According to the carbonate rock classification proposed by Folk [30] and Dunham [31], the Tr_2 sample can be classified as micrite and mudstone, respectively.

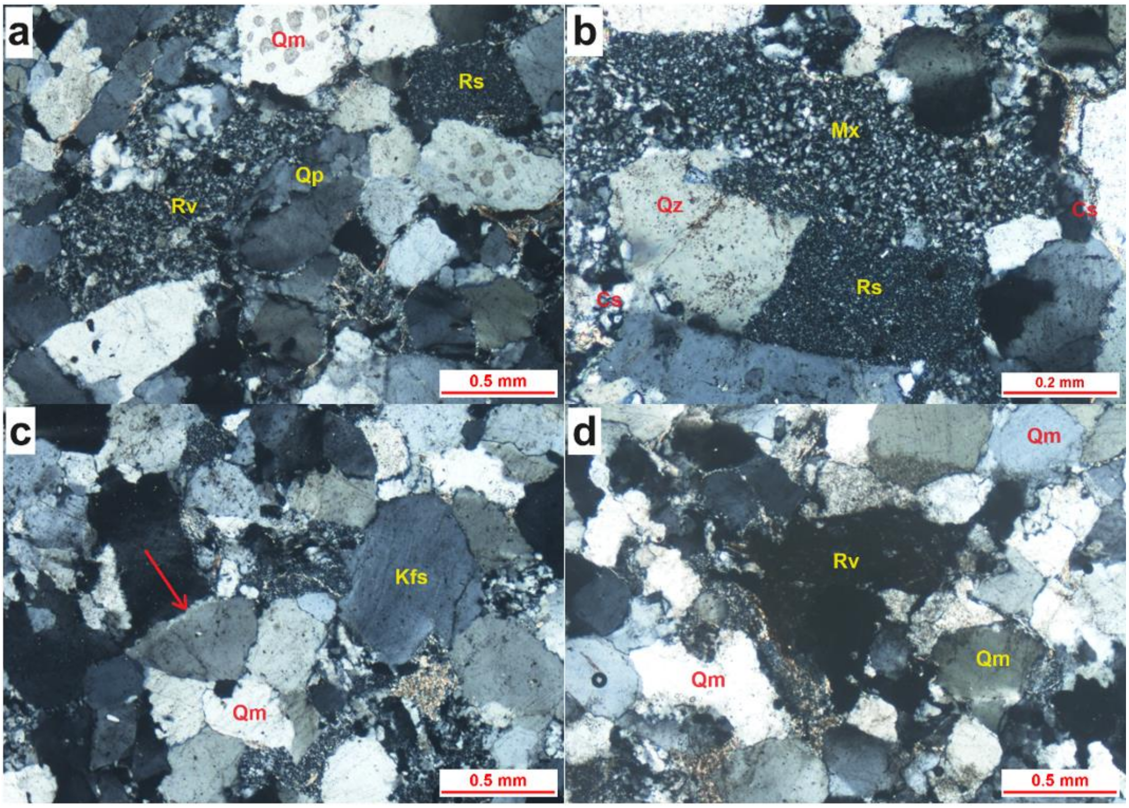

Figure 2 Photomicrographs of Tr_1 sandstone taken under crossed-polarized light. (a) Tr_1-1 showing monocrystalline (Qm) and polycrystalline quartz (Qp) associated with fragments of a siliceous rock (Rs) and a volcanic rock (Rv). (b) At high magnification, the rock matrix (Mx) is associated with clasts of quartz and volcanic fragments with silica cement (Cs). (c) Tr_1-2 showing clasts of alkali feldspar (Kfs) and monocrystalline quartz associated with recrystallization of microcrystalline quartz along the large grain boundaries (arrow). (d) Clasts of volcanic rocks associated with quartz crystals surrounded by the rock matrix

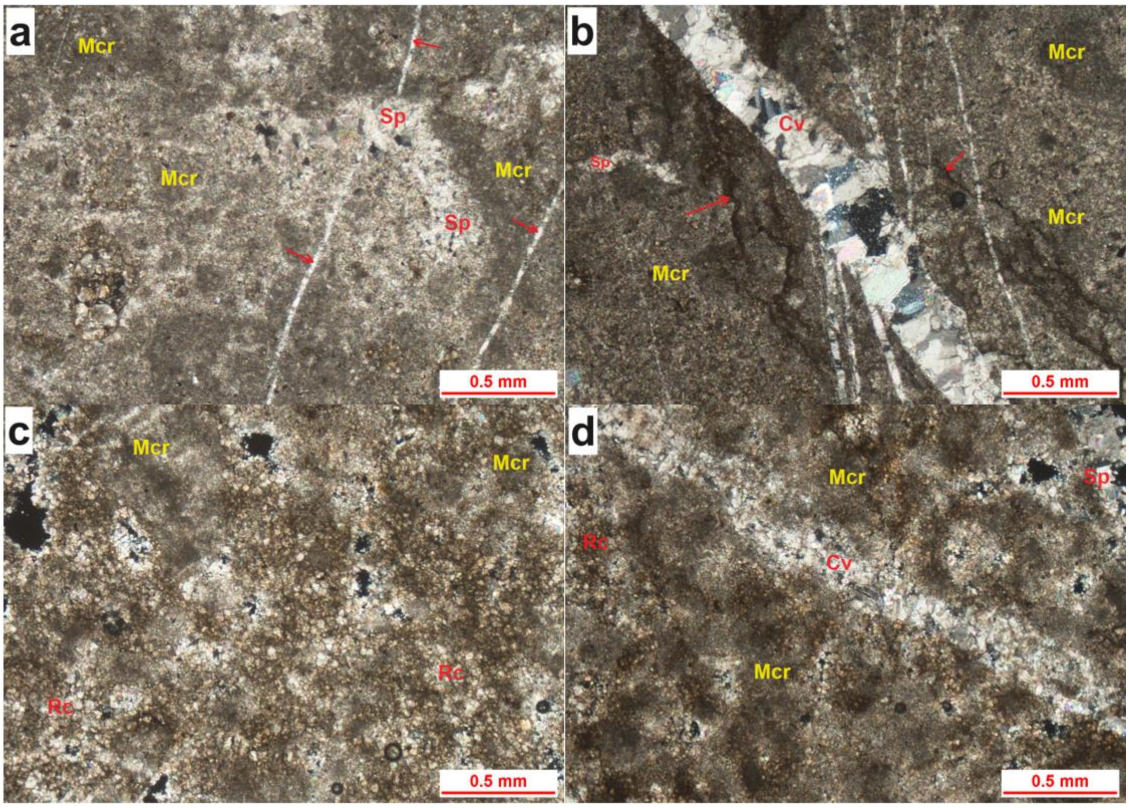

Figure 3 Photomicrographs of Tr_2 limestone taken under crossed-polarized light. (a) Tr_2-1 showing a mud-supported limestone crosscut by calcite veins (arrows). The nearly opaque micrites (Mcr) are dominant in the sample in association with transparent-to-translucent sparite (Sp). (b) Fe hydroxide veinlets (arrows) and calcite veins (Cv) crosscutting the original rock. (c) Tr_2-2 showing calcareous particles of micrites and secondary recrystallized carbonates (Rc). (d) The sample is crosscut by a 0.3 mm-thick calcite vein

Microscopically, the sandstone of Tr_3 shows matrix-supported textures with poor sorting. The grains are made up of 58.25–61.75% of the rock components exhibiting highly angular to angular shapes with low-to-high sphericity (Figure 4). An average grain size ranges from 0.06 to 1.6 mm, defined as very coarse-to-fine sand. The types of grains include crystal clasts (15.5–23%), rock fragments (35.25–46%), and detrital minerals (0.25%). The crystals comprise 4.75–8.25% quartz and 10.75–15.75% plagioclase feldspars. The clasts of rock fragments indicate volcanic-to-pyroclastic rocks containing rich and poor amounts of opaque minerals. The detrital clasts are muscovite and amphibole. These clasts are surrounded by fine-grained matrixes (13–13.25%) and cements (23.75–26.5%). The cements can be found as carbonate and silica with percentages of 23–25.75% and 0.75%, respectively. Secondary opaque minerals are found at approximately 1.625%. According to the classification proposed by Pettijohn [29], the Tr_3 has been classified as lithic greywacke.

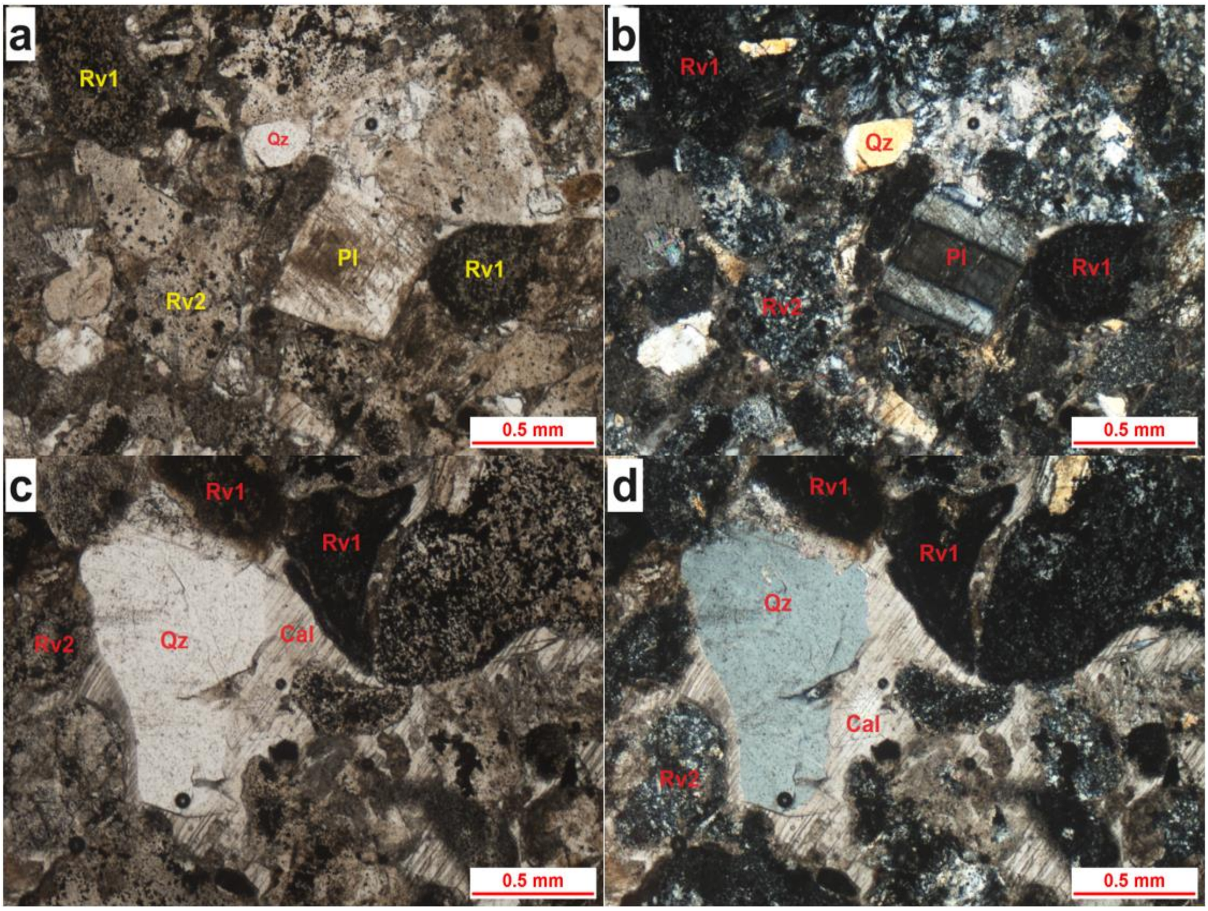

Figure 4 Photomicrographs of Tr_3 samples exhibiting a poorly sorted, matrix-supported structure. (a) Angular-to-subangular grains comprise single quartz (Qz) and plagioclase (Pl) crystals associated with two types of rock fragments (Rv1, Rv2). (b) The corresponding image taken under crossed-polarized light shows the opaque mineral-rich volcanic rock fragments indicated by Rv1, whereas those of poor in opaques are indicated by Rv2. (c) Clasts of quartz and rock fragments are surrounded by calcite cements (Cal). (d) Corresponding image taken under crossed-polarized light

The sample of Tr_4 is predominantly matrix-supported limestones composed of carbonate matrixes (micrites) in a total amount of 44.5–44.75% of the whole rock components associated with 8.75–17.25% carbonate clasts or allochems as shown in Figure 5. The allochems observed here include bioclasts, carbonate lumps, and peloids. Most of them are observed as bioclasts (6.25–12.25%) exhibiting fossils of gastropods and crinoid stems. These allochems range from 0.2 to 0.6 mm in diameter and could be up to 3 mm. The peloids, on the other hand, exhibit muddy micritic features forming spherical-to-oval shapes having a diameter of less than 0.1 mm. Around 19.75–22.5% are small-sized sparry calcites, known as microsparites or recrystallized micrites. The microsparites are 0.1–0.5 mm in diameter. Additionally, calcite veins are locally observed having a thickness ranging from 0.1 to 1.5 mm. According to the carbonate rock classification proposed by Folk [30] and Dunham [31], the sample can be named biomicrite and wackestone, respectively.

3.3 Equivalent quartz content

The equivalent quartz content was obtained by the calculation of the modal mineral percents and their relative Rosiwal hardness values. The hardnesses of quartz, feldspar, calcite, and clay minerals, have been calculated from *equation 2*. The results suggested that they are equal to 104.3, 40.3, 2.3, and 1.4, respectively. The hardness values of rock fragments in the samples of Tr_1 and Tr_3 were roughly estimated based on their mineral contents. The average EQC values of the samples are presented in Table 4.

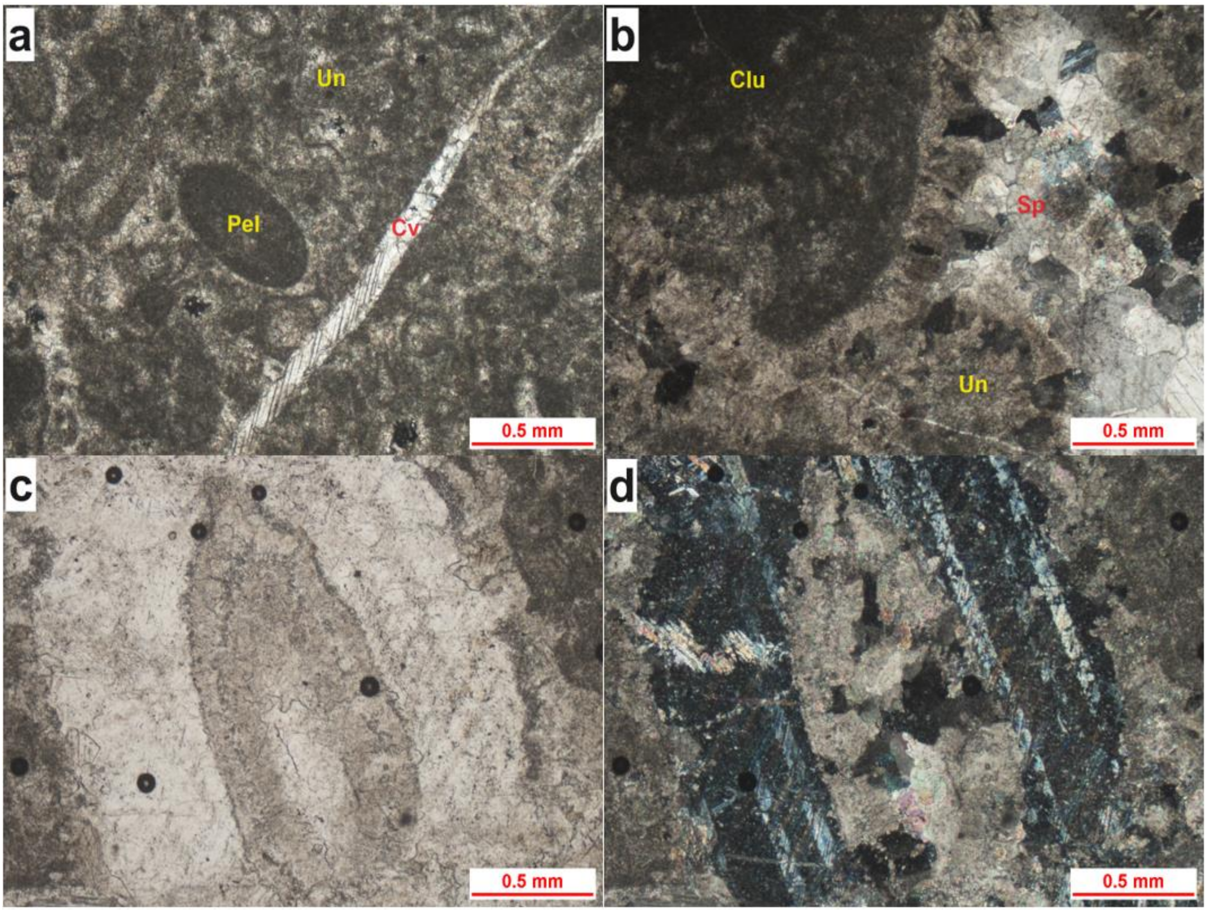

Figure 5 Photomicrographs of Tr_4 samples exhibiting a biomicritic limestone or wackestone. (a) The allochems including peloid (Pel) and unidentified bioclasts (Un) surrounded by a micritic background crosscut by a calcite vein. (b) The occurrence of the large-sized carbonate lump formed is associated with sparite and micrite. (c) The crinoid stem is found as a bioclast that was replaced by calcite crystals. (d) Corresponding image taken under crossed-polarized light

Table 4 Average EQC values of the studied samples obtained from the calculation of their modal mineral contents and Rosiwal scales of hardness

Mineral Phase	Rosiwal Hardness	Mineral composition (%)							
		Tr_1		**Tr_2**		**Tr_3**		**Tr_4**	
		1	2	1	2	1	2	1	2
Amphibole	25.00	-	-	-	-	0.25	-	-	-
Calcite	2.31	-	-	72.25	81.75	23.00	25.75	100	100
Dolomite	3.72	-	-	27.75	18.25	-	-	-	-
Feldspar	40.26	3.25	10	-	-	10.75	14.75	-	-
Micas	1.44	-	-	-	-	-	0.25	-	-
Fe-oxides	40.26	-	-	-	-	1.25	2	-	-
Quartz	104.33	74.75	72.5	-	-	4.75	8.25	-	-
Matrix	52.89	5.25	2.5	-	-	13.25	13	-	-
Cement-cc	2.31	-	-	-	-	23	25.75	-	-
Cement-qz	104.33	5.5	5.75	-	-	0.75	0.75	-	-
Sericite	2.31	3.5	0.75	-	-	-	-	-	-
Rm	52.89	1.5	2.25	-	-	-	-	-	-
Rs	104.33	3.75	4	-	-	-	-	-	-
Rv	72.30	2.5	2.25	-	-	-	-	-	-
Rv1	56.28	-	-	-	-	21.75	15.75	-	-
Rv2	62.59	-	-	-	-	24.25	19.5	-	-
	Total	100.00	100.00	100.00	100.00	100.00	100.00	100.00	100.00
	EQC (%)	90.5	90.1	2.6	2.5	43.7	42.8	2.2	2.2
	Average EQC (%)	**90.3**		**2.6**		**43.3**		**2.2**	

Abbreviation: Rm = metamorphic rock fragments, Rs = siliceous rock fragments, Rv = pyroclastic rock fragments, Rv1 = opaque-poor volcanic rock fragments, Rv2 = opaque-rich volcanic rock fragments

It is clear that the EQC increases with an increasing quartz content of the sample. The arenite (Tr_1) is predominantly composed of 80% quartz components, resulting in the highest EQC value of approximately 90%. Meanwhile, the EQC of the Tr_3 lithic-rich sandstone is half as high due to its lesser quartz content with higher contents of feldspar and volcanic lithic fragments. In addition, the dominant cementing phase of the Tr_3 sample is calcite, whereas those of Tr_1 are silica (quartz). The limestones of Tr_2 and Tr_4 both exhibit relatively low EQC values that are 2.6% and 2.2%, respectively. The slight difference in these values is likely induced by the occurrence of dolomite in the Tr_2 limestone. This study highly agrees that the differences in mineral assemblage and their contents formed in the rock units significantly affect the overall rock hardness, which can be expressed as the EQC. The values of EQC appear to be sufficient for a comparison of hardness among the rock units as a primary rock abrasiveness assessment. However, the EQC values only reflect the mineralogical properties of the rocks and could not be effectively used alone.

3.4 Rock strength

The studied rock samples can be characterized as medium-to-strong strength according to a classification of rock strength proposed by Attewell and Farmer [32]. The rock strength values of each unit resulting from the UCS testing method are presented in Table 5. The lithic-rich sandstone representing the Tr_3 shows the highest average UCS value (92.2 MPa) indicating a strong rock. Tr_1 arenite, on the other hand, has medium-to-high UCS values with an average value of 80.3 MPa despite its highest EQC value. Besides the mineral composition, the strength of rocks is distinctly yielded by rock texture, regional-to-local structure, bedding, fractures/joints, water content, and state of stress. The petrographic results of the Tr_3 sandstone clearly exhibit poorly sorted matrix-supported textures, whereas the Tr_1 shows the opposite feature of clast-supported textures with moderate sorting. These discrete sedimentation textures certainly affect the different UCS values between the two sandstone formations provided by this study. Moreover, the sericite observed in the Tr_1 samples indicates partial alterations of feldspar that possibly reduce the rock strength. In addition, the Tr_2 dolomite-bearing limestone exhibits 77.2 MPa of the average UCS, which is higher than those of the Tr_4 limestone (55.9 MPa). The measured UCS for sandstones and limestones of this study fell into the typical UCS ranges for white-to-brown and grey sandstones and limestones obtained by several previous works [32-35].

Table 5 Average UCS values of the studied samples and the classification based on Attewell and Farmer [32]

Sample	No.	A (mm^2)	P (kN)	UCS (MPa)	Average UCS	Classification
Tr_1	#1	1,287.83	108.9	84.6	**80.3**	Medium
	#2	1,290.80	81.7	63.3		
	#3	1,287.83	119.8	93.0		
Tr_2	#1	1,288.25	110.4	85.7	**77.2**	Medium
	#2	1,288.67	84.7	65.7		
	#3	1,287.40	103.3	80.2		
Tr_3	#1	1,290.80	112.7	87.3	**92.2**	Strong
	#2	1,292.07	116.5	90.7		
	#3	1,292.49	127.6	98.7		
Tr_4	#1	1,291.64	78.3	60.6	**55.9**	Medium
	#2	1,288.67	90.5	70.2		
	#3	1,299.30	47.9	36.9		

3.5 Rock abrasivity index

Once the mineralogical EQC and mechanical UCS parameters have successfully been obtained for all rock samples, the rock abrasivity of each unit could be revealed as calculated through equation 4. The RAI of the studied samples are shown in Table 6. Unsurprisingly, the sample with the highest RAI (72.5) is found to be the Tr_1 sandstone, indicating a very abrasive rock based on the previous classification by [5, 10]. The RAI of the Tr_3 sandstone, which is nearly 40, is classified as a medium abrasive rock. Two limestone formations of Tr_2 and Tr_4 are not abrasive as they have very low RAI exhibiting 2.0 and 1.2, respectively. The results point out that the RAI distinctly increases with the EQC and UCS values.

Table 6 Rock abrasivity index (RAI) of the studied samples estimated from their average equivalent quartz contents and uniaxial compressive strengths. The rock abrasiveness classification is based on previous works [5, 10]

Sample	Average EQC (%)	Average UCS (MPa)	RAI	Classification
Tr_1	90.3	80.3	72.5	*Very Abrasive*
Tr_2	2.6	77.2	2.0	*Not Abrasive*
Tr_3	43.3	92.2	39.9	*Medium Abrasive*
Tr_4	2.2	55.9	1.2	*Not Abrasive*

These findings support that rock abrasivity is dominantly controlled by formation mineral assemblages and the hardness of those minerals compared to quartz. High contents of quartz or quartz-equivalent minerals affect relatively high values of EQC and thus RAI. Meanwhile, the UCS values are likely dependent on mineralogy, alteration, and rock textures, such as grain size, sorting, and cementation. Higher-degree compositional variation and cementation association with lower-degree alteration certainly increase the strength of sedimentary rocks. The relationships between the modal mineral contents of all studied samples and their relative EQC, UCS, and RAI values are shown in Figure 6.

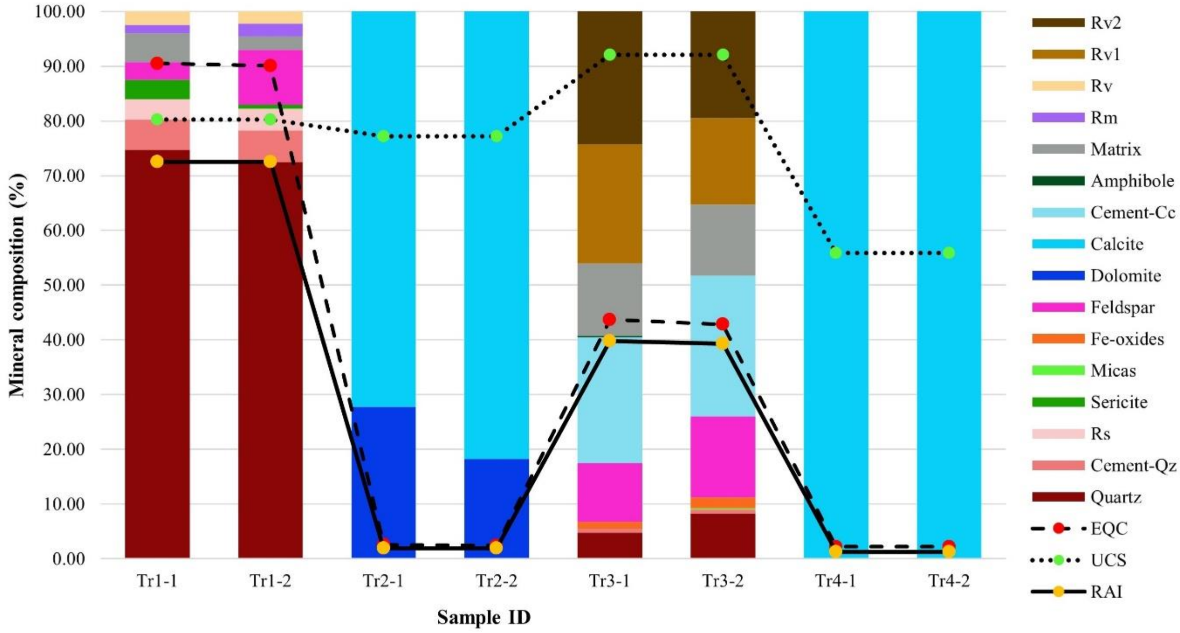

Figure 6 Compositional variations of the studied samples obtained by petrographic analysis and their relative EQC, UCS, and RAI values. The EQC significantly exhibits a positive relationship with quartz content, whereas the UCS increases with increasing mineral variations and cementation

3.6 Implications for tool wear prediction

Evaluation of rock abrasiveness using the rock abrasivity index appears to be an alternative method, which is affordable and effective. The values of RAI can be used as comparative parameters among the different rock types or rock formations, and used in a prediction of tool wear, for instance, an estimation of a drill bit lifetime [5, 10, 25]. The drill bit lifetime, or known as bit lifespan, has a unit of drillable meters per bit (m/bit). Larger drillable distances are caused by the lower abrasive degree of the formations as the wear of drilling bits is low. Extremely abrasive formations, on the other hand, sufficiently induce extremely high-degree bit wear, resulting in relatively low drillable distances.

According to previous works by Plinninger [10] and Thuro [19], they approximated the lifespan of 45 mm-diameter button drill bits based on the formation EQC and RAI values, respectively. Starting with the study of Thuro [19], the author reported that the limestones with below 20% EQC show longer bit lifetimes than the sandstones, which have an EQC of up to 90%. Predicting the lifespan of the 45-mm button drill bit using the EQC of this study indicates that the Tr_1 sandstone significantly causes very high bit wear and provides a short drill bit lifetime of below 500 meters. The EQC of the Tr_3 sandstone also indicates a high damage of the bit, which results in 700 meters per bit. Tr_2 and Tr_4, which are low EQC, both exhibit the longest bit lifetimes (>2,500 m/bit) as the wear of the drill bits is very low. However, it should be noted that these tool wear predictions exclude the determination of rock strength. A later study by Plinninger [5, 10] developed the method for tool wear prediction using the RAI. As the RAI calculation includes both EQC and the rock strength (e.g. UCS), their tool wear prediction was slightly different from the earlier method. Regarding the RAI of this study, the Tr_1 indicates a drillable distance of 500 meters for the 45-mm button drill bit, whereas the bit lifetime of the Tr_3 is nearly 900 meters for the same bit type. The limestones of Tr_2 and Tr_4 have relatively long lifetimes of the drill bit, which are nearly 1,900 meters.

Estimating the number of drill bits required for drilling a particular formation accounts for the lifetime of a selected drill bit and a preferred drilling distance or the formation thickness. This study attempted this calculation by using the predicted drill bit lifetime based on the RAI of the rock samples and their formation thickness obtained from earlier geological reports. The overall thickness of Tr_1, Tr_2, Tr_3, and Tr_4 are 650 m, 640 m, 700 m, and 230 m respectively [26-28]. Indeed, this study assumed that the drilling started at the top of the Tr_4 formation moving downward and ended at the bottom of the Tr_1 formation using the 45 mm button bits. The percentages of the full working potential of each drill bit are then estimated from the formation thickness and its life span in the drilling of that formation. The results showed that the first bit has spent only 12.1% of its full working potential for drilling through the Tr_4 formation and spent another 77.8% to drill through the Tr_3. Next, at least 33% of the working potential of the bit is required in the drilling of the Tr_2. This means the first bit apparently reached its maximum efficiency (100%) and needed to be replaced by a new bit for successfully drilling through the formation of the Tr_2. The second bit continued to drill into the Tr_1 with approximately 76% of its working performance. However, the thickness of the Tr_1 is larger than the bit lifespan, which means it requires more than one bit to drill through this formation. The formation requires drill bits with 130% of the working potential. The third bit was then introduced to the Tr_1 to complete this given drilling scenario. Despite the drilling through various geologic stratigraphic formations, the drilling of a single formation could also be required for underground bench excavation, drill-and-blast tunneling, rock supports, or blast-hole drilling. Changing drill bit types and diameter sizes certainly affect the drill bit lifespan of each formation.

This study supports that the RAI provides the smallest-scale geotechnical parameter for estimating tool consumption and wear prediction. Larger-scale relevant parameters analyzed through any simplified tools, particularly the CERCHAR abrasivity index (CAI) should be further considered for increasing confidence in the formation interpretation processes. This method simply tests the rock abrasiveness by directly scratching a sample surface with a defined steel needle over a given distance under a static load [9, 36]. The wear of the needle tip after scratching has been analyzed and used to derive the CAI value. It has earlier been reported that the CAI values show fair correlations to the EQC and UCS [e.g. 11, 37-41]. More studies related to the CAI testing of these samples significantly provide insights into rock abrasiveness assessment that could be compared to the RAI and other relevant techniques.

4. Conclusion

The rock abrasivity assessment of the four stratigraphic formations of the Lampang Group proposed in this study has been achieved through the conventional petrographic analysis coupled with the UCS testing method. The findings of this study are provided as follows.

- Petrographic analysis can be used for an assessment of rock abrasivity that could be applied in mining activities and tunneling or underground constructions. It provides crucial mineralogical parameters and comprehensive details regarding rock textures, mineral content, grain size, and alteration features, which mainly affect the rock strength and overall hardness. This technique should be widely accepted for its convenience, simplicity, and affordable cost.
- The most abrasive formation of the lower Lampang Group is found to be the sandstone of Phra That (Tr_1) Formation as it is classified as very abrasive rock with the highest RAI values. Meanwhile, the non-abrasive units, which exhibit the lowest RAI, are found to be the limestones of Pha Kan (Tr_2) and Doi Long (Tr_4) Formation.
- The rock abrasivity is distinctly controlled by the mineral assemblage of the formations, the mineral hardnesses compared to quartz, and rock strength. The high values of quartz content and the moderate-to-high values of rock strength have been predicted that the formation is very abrasive and positively causes an extreme tool wear.
- The range of RAI values could be used to primarily estimate the number of tool consumption in drilling or excavating activities by predicting the tool lifetime. However, the total thickness of the target formations and preferred drilling distances must be known. The formations having relatively high RAI values tend to reduce the tool lifetime as they extremely affect the tool wear. Responding to this concern, replacement of that eroded tool with a new tool is necessary. Understanding these geologic formation characteristics at microscales is an important step leading to a proper decision for further strategies in mining and/or underground construction processes.

5. Acknowledgements

This study was supported by the Faculty of Engineering, Chiang Mai University. The authors also thank Piyanat Arin for his assistance on petrographic works.

6. References

[1] Capik M, Yilmaz AO. Correlation between Cerchar abrasivity index, rock properties, and drill bit lifetime. Arab J Geosci. 2017;10:1-12.
[2] Torrijo FJ, Garzón-Roca J, Company J, Cobos G. Estimation of Cerchar abrasivity index of andesitic rocks in Ecuador from chemical compounds and petrographical properties using regression analyses. Bull Eng Geol Environ. 2019;78(4):2331-44.
[3] Abu Bakar MZ, Majeed Y, Rashid MA. Influence of propeller material hardness, testing time, rock properties, and conditioning on LCPC rock abrasiveness test. Bull Eng Geol Environ. 2021;80:1599-616.
[4] Li Q, Li J, Duan L, Tan S. Prediction of rock abrasivity and hardness from mineral composition. Int J Rock Mech Min Sci. 2021;140:104658.
[5] Plinninger RJ. Klassifizierung und Prognose von Werkzeugverschleiß bei konventionellenGebirgslösungsverfahren im Festgestein. Münchner Geologische Hefte, Reihe B: Angewandte Geologie. 2002;B17:1-146. (In German)
[6] Plinninger RJ, Spaun G, Thuro K. Prediction and classification of tool wear in drill and blast tunnelling. In: van Rooy JL, Jermy CA, editors. Engineering Geology for Developing Countries - Proceedings of 9th Congress of the International Association for Engineering Geology and Environment; 2002 Sep 16-20; Durban, South Africa. p. 2226-36.
[7] Plinninger RJ. Abrasiveness assessment for hard rock drilling. Geomech Tunnelbau. 2008;1(1):38-46.
[8] Plinninger RJ, Restner U. Abrasiveness testing, Quo Vadis? - a commented overview of abrasiveness testing methods. Geomech Tunnelbau. 2008;1(1): 61-70.
[9] Thuro K, Käsling H. Classification of the abrasiveness of soil and rock. Geomech Tunnelbau. 2009;2(2):179-88.
[10] Plinninger RJ. Hardrock abrasivity investigation using the Rock Abrasivity Index (RAI). In: Williams AL, editor. Geologically Active. London: Taylor & Francis; 2010. p. 3445-2.
[11] Kathancharoen N, Fuenkajorn K. Effects of mechanical and mineralogical properties on CERCHAR abrasivity index and specific energy of some Thai rocks. Eng Appl Sci Res. 2023;50(5):478-89.
[12] Farhadian A, Ghasemi E, Hoseinie SH, Bagherpour R. Prediction of Rock Abrasivity Index (RAI) and Uniaxial Compressive Strength (UCS) of granite building stones using nondestructive tests. Geotech Geol Eng. 2022;40:3343-56.
[13] Shi X, Tang Y, Chen S, Gao L, Wang Y. Experimental study on the sandstone abrasiveness via mineral composition and microstructure analysis. Petroleum. 2023;10(3):440-5.
[14] Hassanpour J, Rostami J, Tarigh Azali S, Zhao J. Introduction of an empirical TBM cutter wear prediction model for pyroclastic and mafic igneous rocks: a case history of Karaj water conveyance tunnel, Iran. Tunn Undergr Space Technol. 2014;43:222-31.
[15] Macias FJ, Dahl F, Bruland A. New rock abrasivity test method for tool life assessments on hard rock tunnel boring: The Rolling Indentation Abrasion Test (RIAT). Rock Mech Rock Eng. 2016;49(5):1679-93.
[16] Kaspar M, Latal C. Der äquivalente Quarzgehalt – Historischer Rückblick und seine Zukunft in der Anwendung der Abrasivitätsprognose. Geotechnik. 2022;45(2):86-97. (In German)
[17] Rosiwal A. Neuere Ergebnisse der Härtebestimmung von Mineralien und Gesteinen. - Ein absolutes Maß für die Härte spröder Körper. Verhandlungen der k. k. geologischen Reichsanstalt; 1916; Wien. p. 117-47. (In German)
[18] Schimazek J, Knatz H. Die Beurteilung von Gesteinen durch Schneid- und Rollenbohrwerkzeuge. Erzmetall. 1976;29:113-19. (In German)
[19] Thuro K. Drillability prediction: geological influences in hard rock drill and blast tunnelling. Geol Rundsch. 1997;86:426-38.
[20] Verhoef PN. Wear of rock cutting tools: implications for the site investigation of rock dredging projects. Rotterdam: CRC Press; 1997.
[21] Golodkovskaia GA, Krasilova NS, Ladygin VM, Shaumian LV. Factors controlling solid rock strength. Bull Int Assoc Eng Geol. 1975;11:65-9.

[22] Bieniawski ZT, Bernede MJ. Suggested Methods for determining the uniaxial compressive strength and deformability of rock materials: part 1. Suggested method for determining deformability of rock materials in uniaxial compression. Int J Rock Mech Min Sci Geomech Abstr. 1979;16(2):138-40.
[23] ASTM. ASTM D2938-95: Standard test method for unconfined compressive strength of intact rock core specimens. West Conshohocken: American Society for Testing and Materials; 2017.
[24] ISRM. Suggested methods for determining point load strength. Int J Rock Mech Min Sci Geomech Abstr. 1985;22(2):51-60.
[25] Beckhaus K, Thuro K. Abrasivität von Lockergestein in der Großbohrtechnik: Versuchstechnik und praktische Erfahrungen. 30 Baugrundtagung; 2008 Sep 24-27; Dortmund, Germany. Essen: Deutsche Gesellschaft für Geotechnik; 2008. p. 171-80. (In German)
[26] Chaodumrong P. Stratigraphy, sedimentology and tectonic setting of the Lampang Group, central north Thailand [dissertation]. Tasmania: University of Tasmania; 1992.
[27] Chaodumrong P, Burrett CF. Stratigraphy of the Lampang Group in central north Thailand: new version. CCOP Technical Bulletin. 1997;26:65-80.
[28] Charusiri P, Ratanasthien B, Karnchanapayom P, Chaernthitirat T, Pailoplee S, Chitrmahantakul S, et al. Consulting, review, and evaluation geology Mae Moh Mine. Final report. Lampang, Thailand: Electricity Generating Authority of Thailand; 2020.
[29] Pettijohn FJ. Sedimentary rocks. 2nd ed. New York: Harper and Row Publishers; 1975.
[30] Folk RL. Practical petrographic classification of limestones. AAPG Bulletin. 1959;43:1-38.
[31] Dunham RJ. Classification of carbonate rocks according to depositional texture. In: Ham WE, editor. Classification of Carbonate Rocks. Tulsa: AAPG; 1962. p. 108-21.
[32] Attewell PB, Farmer IW. Principles of engineering geology. London: Chapman and Hall; 1976.
[33] Ozturk CA, Nasuf E. Strength classification of rock material based on textural properties. Tunn Undergr Space Technol. 2013;34:45-54.
[34] Dweirj M, Fraige F, Alnawafleh H, Titi A. Geotechnical characterization of Jordanian limestone. Geomaterials. 2017;7:1-12.
[35] Huang S, He Y, Yu S, Cai C. Experimental investigation and prediction model for UCS loss of unsaturated sandstones under freeze-thaw action. Int J Min Sci Technol. 2022;32(1):41-9.
[36] Ko TY, Kim TK, Son Y, Jeon S. Effect of geomechanical properties on Cerchar Abrasivity Index (CAI) and its application to TBM tunnelling. Tunn Undergr Space Technol. 2016;57:99-111.
[37] Suana M, Peters T. The Cerchar Abrasivity Index and its relation to rock mineralogy and petrography. Rock Mechanics. 1982;15:1-8.
[38] West G. Rock abrasiveness testing for tunnelling. Int J Rock Mech Min Sci Geomech Abstr. 1989;26(2):151-60.
[39] Al-Ameen SI, Waller MD. The influence of rock strength and abrasive mineral content on the Cerchar Abrasive Index. Eng Geol. 1994;36(3-4):293-301.
[40] Plinninger RJ, Käsling H, Thuro K, Spaun G. Testing conditions and geomechanical properties influencing the CERCHAR abrasiveness index (CAI) value. Int J Rock Mech Min Sci. 2003;40(2):259-63.
[41] Zhang SR, She L, Wang C, Wang YJ, Cao RL, Li YL, et al. Investigation on the relationship among the Cerchar abrasivity index, drilling parameters and physical and mechanical properties of the rock. Tunn Undergr Space Technol. 2021;112:103907.